Blocking Double-Stranded RNA-Activated Protein Kinase PKR by Japanese Encephalitis Virus Nonstructural Protein 2A

Yu-Chun Tu,[a,c] Chia-Yi Yu,[c] Jian-Jong Liang,[c] Elong Lin,[c,e] Ching-Len Liao,[a,b] and Yi-Ling Lin[a,b,c,d]

Graduate Institute of Life Sciences[a] and Department of Microbiology and Immunology,[b] National Defense Medical Center, Taipei, Taiwan; Institute of Biomedical Sciences[c] and Genomics Research Center,[d] Academia Sinica, Taipei, Taiwan; and Department of Food Science and Technology, Central Taiwan University of Science and Technology, Taichung, Taiwan[e]

Japanese encephalitis virus (JEV) is an enveloped flavivirus with a single-stranded, positive-sense RNA genome encoding three structural and seven nonstructural proteins. To date, the role of JEV nonstructural protein 2A (NS2A) in the viral life cycle is largely unknown. The interferon (IFN)-induced double-stranded RNA (dsRNA)-activated protein kinase (PKR) phosphorylates the eukaryotic translation initiation factor 2α subunit (eIF2α) after sensing viral RNA and results in global translation arrest as an important host antiviral defense response. In this study, we found that JEV NS2A could antagonize PKR-mediated growth inhibition in a galactose-inducible PKR-expressing yeast system. In human cells, PKR activation, eIF2α phosphorylation, and the subsequent translational inhibition and cell death triggered by dsRNA and IFN-α were also repressed by JEV NS2A. Moreover, among the four eIF2α kinases, NS2A specifically blocked the eIF2α phosphorylation mediated by PKR and attenuated the PKR-promoted cell death induced by the chemotherapeutic drug doxorubicin. A single point mutation of NS2A residue 33 from Thr to Ile (T33I) abolished the anti-PKR potential of JEV NS2A. The recombinant JEV mutant carrying the NS2A-T33I mutation showed reduced *in vitro* growth and *in vivo* virulence phenotypes. Thus, JEV NS2A has a novel function in blocking the host antiviral response of PKR during JEV infection.

The interferon (IFN)-induced double-stranded RNA (dsRNA)-activated protein kinase (PKR) plays a critical role in host antiviral defense. PKR is an antiviral IFN-stimulated gene (ISG) (24, 55) and also is a pathogen recognition receptor (PRR) (31) recognizing dsRNA for IFN induction. The inactive form of PKR is a monomer with two dsRNA-binding domains and one catalytic domain. dsRNA binding promotes PKR dimerization, autophosphorylation, and then phosphorylation of its substrate, eukaryotic translation initiation factor 2α subunit (eIF2α) (16, 64). eIF2 is composed of three subunits (α, β, and γ). In its GTP-bound form, eIF2 mediates the transfer of initiator methionyl-tRNA to the 40S ribosomal subunit. Once the initiation is completed, eIF2, in its GDP-bound form, is released from the ribosome. To participate in another round of translation initiation, eIF2-GDP must be converted to eIF2-GTP by eIF2B. The activity of eIF2 is regulated by phosphorylation at Ser51 of its α subunit. Once eIF2α is phosphorylated, binding of eIF2 and eIF2B increases greatly, thus leading to a competitive inhibition of the eIF2B-mediated eIF2 GDP-GTP exchange reaction. Because cellular eIF2B is present in limited amounts, sequestering eIF2B results in aborted translation initiation and global translation blockage of both cellular and viral mRNA (3, 30). Therefore, PKR functions as a host antiviral defense mechanism and various viruses have evolved diverse strategies to escape PKR activation (28, 29).

Japanese encephalitis virus (JEV) is a mosquito-borne flavivirus that causes acute encephalitis with high mortality, especially in Asia. Other members of the *Flavivirus* genus of the family *Flaviviridae*, such as West Nile virus (WNV), dengue virus (DENV), and yellow fever virus (YFV) also cause serious medical problems in humans. Although PKR has been viewed as having a host antiviral function, its roles among the members of *Flaviviridae* family vary. PKR can serve as a PRR to mediate IFN production in WNV infection (31), and antiviral effects of PKR against WNV have been demonstrated in both cell culture systems (36) and challenged animals (58). Nevertheless, other studies have shown that PKR is dispensable for IFN-mediated inhibition of DENV replication (17, 36). Moreover, both antiviral and proviral roles of PKR have been reported for hepatitis C virus (HCV), a member of the *Flaviviridae* family. The proviral effect was achieved because PKR activation inhibits translation of cellular antiviral IFN effectors, whereas HCV mRNA translates through its internal ribosome entry site (IRES) that is resistant to PKR activation (1, 2, 27). PKR has also been shown to inhibit HCV replication (35) and HCV E2 and NS5A proteins appear to block PKR activation (23, 25, 26, 59, 60). Among the PKR inhibition determinants of HCV, the IFN sensitivity-determining region (ISDR) of NS5A has been studied extensively for its molecular mechanism of binding to PKR (23).

JEV viral particles are enveloped and contain a positive-sense RNA genome that encodes a polyprotein. By posttranslational processing, three structural proteins (core [C], precursor of membrane [prM], and envelope [E]) and seven nonstructural proteins (NS1, NS2A, NS2B, NS3, NS4A, NS4B, and NS5) are produced from flaviviral polyprotein. Flavivirus NS2A is a small hydrophobic transmembrane protein, and thus far the role of JEV NS2A (JNS2A) in the viral life cycle remains largely unknown. Studies of other flaviviruses have suggested roles of flaviviral NS2A in modulating viral assembly and host IFN system. Kunjin virus (KUNV) NS2A associates with viral RNA (51) and is involved in blocking IFN induction and signaling during KUNV and WNV infection

(48–50). NS2A of YFV and KUNV play a role in virus assembly and/or infectious virus particle secretion (39, 40, 47).

In this study, we used a functional assay in a yeast system and found a novel role of JNS2A in blocking PKR-mediated growth repression. We further demonstrated the anti-PKR potential of JNS2A in mammalian cells treated with several stimuli known to activate PKR. A single amino acid of JNS2A, Thr at residue 33, was found important for its PKR-suppressing effect, and a Thr-to-Ile substitution of this residue of NS2A hampered both the *in vitro* growth and *in vivo* virulence phenotypes of JEV infection. The involvement of JEV NS2A in modulating the important host antiviral molecule PKR is presented and discussed.

MATERIALS AND METHODS

Cells, viruses, and chemicals. The human lung carcinoma A549 and human kidney 293T cells were cultured in 10% fetal bovine serum (FBS; Gibco) and 2 mM L-glutamine (Gibco) containing F-12 (Gibco) and Dulbecco modified Eagle medium (DMEM; Gibco), respectively. Baby hamster kidney fibroblast BHK-21 cells were cultured in RPMI 1640 medium containing 5% FBS and 2 mM L-glutamine. A549 cells with green fluorescent protein (GFP), JNS2A, or PKRΔ6 stable expression were generated by pTY-EF1α (7, 14, 34) lentiviral transduction according to the protocols provided by Taiwan National RNAi Core Facility (63). The lentiviral vectors expressing the shRNA targeting human PKR (5'-GAGGCGAGAAA CTAGACAAAG-3', TRCN0000197012) and control LacZ (5'-TGTTCG CATTATCCGAACCAT-3', TRCN0000072223) were from the Taiwan National RNAi Core Facility. JEV RP-9 strain (10) (GenBank accession no. AF014161) was propagated in mosquito C6/36 cells with RPMI 1640 medium (Gibco) containing 5% FBS. JNS2A-T33I mutated virus was generated by a single primer cloning method (52) with the primer 5'-GTGG ACGGCCAGATTGA$\underline{T}$CATTCCTGCGGTTTTGG-3' (the mutated sequence is underlined) using a JEV infectious clone as previously described (42). Poly(I·C) (low molecular weight) was obtained from Invivogen, and doxorubicin hydrochloride was from Sigma.

Virus infection and titration. Viral infection and titration were as previously described (42). Briefly, cells were adsorbed with virus at the indicated multiplicity of infection (MOI) for 2 h, washed, and incubated at 37°C. The culture supernatants were collected, and virus titers were determined by plaque-forming assay in BHK-21.

Plasmid construction. The cDNA fragments encoding individual JEV proteins (44) were subcloned into the galactose-inducible yeast-bacterial shuttle vector pYES2 (Invitrogen) under the GAL1 and T7 promoters. To generate lentiviral constructs, hemagglutinin (HA)-tagged JNS2A, GFP, and PKRΔ6 (38, 57) were cloned into pTY-EF1α. The bicistronic reporter CMV-FLuc$_{d2}$-IRES$_{HCV}$-RLuc was constructed by inserting a firefly luciferase (FLuc) C-terminally tagged with PEST sequences (d2) that enhance protein degradation (41, 56) under a cytomegalovirus (CMV) immediate-early (IE) promoter. *Renilla* luciferase (RLuc) driven by HCV IRES (HCV 5' untranslated region [UTR] and 36 nucleotides [nt] of the Core gene) was then placed downstream of the CMV-driven FLuc$_{d2}$. All constructs were checked by DNA sequencing.

Rescue of PKR-repressed yeast growth assay. Yeast *Saccharomyces cerevisiae* strain RY1-1 (*MAT***a** *ura3-52 leu2-3 leu2-112 gcn2Δ trp1-Δ63 LEU2*::[*GAL-CYC1-PKR*]$_2$), which contains two integrated copies of human PKR under the control of galactose-inducible *GAL1-CYC1* promoter (25, 57, 60), was kindly provided by Alan G. Hinnebusch (National Institute of Child Health and Human Development, Bethesda, MD). The yeast plasmids pYES2 encoding individual JEV viral proteins, HIV-Tat (a positive control) (6), and vector only (for negative control) were introduced into yeast strain RY1-1 by the lithium acetate procedure (5, 11). Briefly, plasmid DNA (1 μg) and carrier salmon sperm DNA (20 μg) were mixed with RY1-1, and then 500 μl of PLATE mixture (1 M lithium acetate [pH 7.5], 45% PEG 4000, 1 M Tris-HCl [pH 7.5], 0.5 M EDTA [pH 8.0]) and 20 μl of 1 M dithiothreitol were added and mixed. After incubation at

room temperature for 8 h and 42°C heat shock for 10 min, yeast cells were incubated in synthetic dextrose (SD; without uracil) medium containing 2% glucose, 0.01% tryptophan, and 0.67% yeast nitrogen base (with ammonium sulfate) for 4 days at 30°C. For PKR-mediated growth suppression assay, the yeast transformants were streaked onto plates of synthetic galactose (SGAL; without uracil) containing 2% galactose, 0.01% tryptophan, and 0.67% yeast nitrogen base (with ammonium sulfate) to induce PKR-mediated phosphorylation of eIF2α. To monitor the growth kinetics, individual yeast colonies were inoculated in SD broth at 30°C overnight and then diluted to an optical density at 600 nm (OD$_{600}$) of 0.4/ml in SGAL (10% galactose) broth, and cell growth at 30°C was monitored by spectrometer (OD$_{600}$).

PKR activation and cell survival assay. PKR was activated by poly(I·C) transfection with Lipofectamine 2000 (Invitrogen), IFN-α2a (Roferon-A; Roche), and doxorubicin hydrochloride treatments. Viable cell numbers were determined by the trypan blue exclusion method. Cell survival was also evaluated by staining with annexin V-fluorescein isothiocyanate (annexin V-FITC) and propidium iodide (PI; BioVision) for 5 min in the dark. Stained cells were analyzed by FACSCanto flow cytometry and FACSDiva software (Becton Dickinson).

Western blot analysis. Western immunoblotting was performed as described previously (43). Briefly, equivalent amounts of total proteins (lysed with sodium dodecyl sulfate [SDS] lysis buffer composed of 62.5 mM Tris-HCl [pH 6.8], 2% SDS, 10% glycerol, and protease/phosphatase inhibitors; Roche) were separated by SDS-PAGE and transferred to nitrocellulose membrane (Hybond-C Super; Amersham). After blocking with 5% bovine serum albumin or skim milk in TBS-T, the membranes were probed with primary antibodies and horseradish peroxidase (HRP)-conjugated secondary antibody (Jackson Immunoresearch) and then developed with an enhanced chemiluminescence system (Pierce). The rabbit polyclonal anti-PKR (catalog no. 3072), anti-eIF2α (catalog no. 9722), anti-phospho-eIF2α (Ser51, catalog no. 9721), and monoclonal anti-HA tag (catalog no. 3724) antibodies were obtained from Cell Signaling. The anti-phospho-PKR (pT446) rabbit monoclonal antibody (catalog no. 1120-1) was from Epitomics. Mouse monoclonal antibodies specific for JEV NS1 and NS3 were as described previously (9), and mouse anti-actin antibody was from Chemicon.

Immunoprecipitation-Western blot assay. 293T cells were cotransfected with Flag-tagged PKRΔ6 plus HA-tagged JEV NS2A or NS2A-T33I or with V5-tagged PKR or LacZ (Invitrogen) plus HA-tagged NS2A or NS2A-T33I with Lipofectamine 2000 (Invitrogen) for 24 h. The cells were rinsed with phosphate-buffered saline (PBS) and lysed with protein lysis buffer (1% NP-40, 1% Triton X-100, 150 mM NaCl, 50 mM Tris-HCl [pH 7.5], 1 mM EDTA) containing a cocktail of protease and phosphatase inhibitors (Roche). Cell lysates were immunoprecipitated with anti-HA affinity gel (E6779; Sigma), anti-Flag M2 affinity gel (A2220; Sigma), or anti-V5 antibody (V8012; Sigma) overnight at 4°C. The immunocomplex was washed three times with protein lysis buffer at 4°C for 30 min and resuspended in sample buffer without 2-mercaptoethanol. Proteins were separated with 4 to 12% NuPage (Invitrogen) and detected with anti-Flag (F7425; Sigma), anti-HA (catalog no. 3724; Cell Signaling), and anti-V5 (V8137; Sigma) antibodies.

IFA. Immunofluorescence assay (IFA) was performed as previously described (63). Briefly, cells were blocked with skim milk in PBS-T after fixation and permeabilization. Anti-HA tag antibody (catalog no. 3724; Cell Signaling) and secondary antibodies conjugated with Alexa Fluor 488 (Invitrogen) were used. The cells were observed and photographed with an inverted fluorescence microscope.

Reporter assay. The bicistronic reporter CMV-FLuc$_{d2}$-IRES$_{HCV}$-RLuc was cotransfected with HA-GFP, -J2A, or -PKRΔ6 in A549 or 293T cells with PolyJet transfection reagent (SignaGen Laboratories). At 24 h after transfection, IFN-α2a (2,000 U/ml) was added for 16 h of stimulation. The activity of FLuc (CMV promoter-driven) and RLuc (HCV IRES-driven for internal control) was measured by using a dual-luciferase assay system (Promega), and the FLuc activity was normalized to that of RLuc.

A. A549

B. 293T
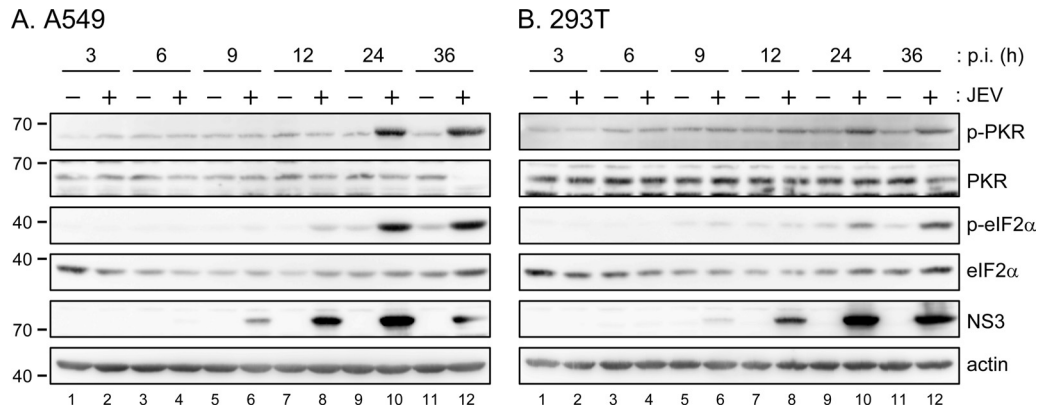
FIG 1 Phosphorylation of eIF2α and PKR was detected late during JEV infection. Human A549 (A) and 293T (B) cells were infected with JEV RP-9 strain (MOI = 5) for the indicated times. The cell lysates were collected and analyzed by Western blotting with the indicated antibodies.

JEV virulence test. RP-9 wild-type and recombinant JNS2A T33I-mutated JEVs were compared for virulence in C57BL/6 mice. Groups of 7-week-old mice were challenged by intraperitoneal inoculation with JEV and intracerebral injection with 30 μl of PBS as described previously (10, 32, 45).

Quantitative reverse transcription-PCR (RT-qPCR). Total RNA was extracted with an RNeasy minikit (Qiagen) and reverse transcribed to cDNA with random hexamer using the ThermoScript RT System (Invitrogen). For quantification, PCR was performed with Power SYBR green PCR Master Mix (Applied Biosystems) according to the manufacturer's instructions. Specific primers for the detection of JEV (5′-AAGTTGAAG GACCAACG-3′ and 5′-GCATGTTGTTGTTTCCAC-3′), human IFN-β (5′-CACGACAGCTCTTTCCATGA-3′ and 5′-AGCCAGTGCTCGATG AATCT-3′), murine interleukin-6 (IL-6; 5′-GCTATGAAGTTCCTCTCT GCAAG-3′ and 5′-TTGAGATCTACTCGGCAAACCTA-3′), and β-actin (5′-TCCTGTGGCATCCACGAAACT-3′ and 5′-GAAGCATTTGC GGTGGACGAT-3′) were used. The relative expression levels of each target gene were normalized to that of actin based on the second derivative maximum method (Roche). The melting curves were used to validate the specificities of products.

ELISA. An enzyme-linked immunosorbent assay (ELISA) for detecting serum anti-JEV antibody was performed as previously described (62). Briefly, JEV-infected C6/36 cells in 96-well plate were incubated overnight at 4°C with serially diluted serum samples and then reacted with HRP-conjugated goat anti-mouse IgG. The color was developed with a 3,3′,5,5′-tetramethylbenzidine (TMB) liquid substrate system for membranes (Sigma), and the absorbance at 450 nm was measured on an ELISA reader. A mouse IL-6 ELISA kit (Thermo, catalog no. EM2IL6) was performed according to the manufacturer's instructions.

RESULTS

Phosphorylation of eIF2α and PKR was detected at late stages of JEV infection. PKR is an IFN-induced dsRNA-activated protein kinase that phosphorylates eIF2α and results in translation arrest. PKR may function as a host antiviral factor and viruses have developed various mechanisms to overcome its actions (28, 29). To understand the role of PKR in JEV infection, we determined the activation status of endogenous PKR by immunoblotting with antibodies against phosphorylated PKR (Thr446) and its downstream substrate eIF2α (Ser51) in human lung carcinoma A549 and human embryonic kidney 293T cells. In both cells, phosphorylation of PKR and eIF2α was not detected until 24 h of JEV infection, whereas viral protein NS3 expression was readily detected at 9 to 12 h after JEV infection in these cells (Fig. 1), sug-

gesting that JEV might avoid triggering or actively suppress PKR activation at the early stage of infection.

JEV NS2A blocked PKR-mediated growth suppression in PKR-expressing yeast system. To explore the anti-PKR potential of JEV proteins, we used a PKR-inducible yeast system: yeast strain RY1-1 that contains two integrated copies of human PKR under the control of galactose-inducible promoter (57). Human PKR expression in yeast strain RY1-1 inhibits translation initiation and cell growth; thus yeast RY1-1 grows poorly in galactose synthetic (SGAL) medium. The individual cDNAs encoding JEV viral proteins were subcloned into a yeast expression plasmid pYES2, and all expressed the proteins with the expected sizes (Fig. 2A). The yeast strain RY1-1 transformed with JEV viral protein plasmids grew well on an SD (synthetic dextrose) plate which contained 2% glucose, and PKR was not induced (Fig. 2B). However, only RY1-1 transformed with the positive control HIV Tat that has been reported to block PKR (6) and that with JEV NS2A grew on the SGAL plate (Fig. 2C). Similarly, RY1-1 transformed with HIV Tat or NS2A but not vector control grew in SGAL broth (Fig. 2D). Thus, JEV NS2A (JNS2A) showed an ability to rescue the PKR-mediated growth suppression in yeast system.

dsRNA-induced eIF2α phosphorylation and cell death were reduced by JNS2A. To evaluate the anti-PKR potential of JNS2A in mammalian cells, we established a human A549 cell line stably expressing HA-tagged JNS2A (J2A) by lentivirus transduction. A549 cells expressing PKRΔ6, a PKR dominant-negative mutant that lacks of six amino acids in its catalytic domain and cannot phosphorylate eIF2α (38, 57), were also established by lentivirus transduction to serve as an anti-PKR positive control. Cells were treated with the dsRNA analogue poly(I·C) and assessed for their PKR activation by immunoblotting with antibody against phosphorylated eIF2α. Since, compared to the GFP-negative control, eIF2α phosphorylation was lower in cells with JNS2A or PKRΔ6 overexpression (Fig. 3A). Because PKR activation has also been shown to mediate stress-induced cell death (4, 15), we evaluated the ability of JNS2A to block dsRNA-induced cell death. With higher doses of poly(I·C) transfection, the control A549 and GFP cells showed apoptotic characteristics under phase-contrast microscopy, whereas JNS2A cells preserved better cell morphological features (data not shown). Cell viability determined by trypan blue exclusion confirmed that cells with JNS2A expression were
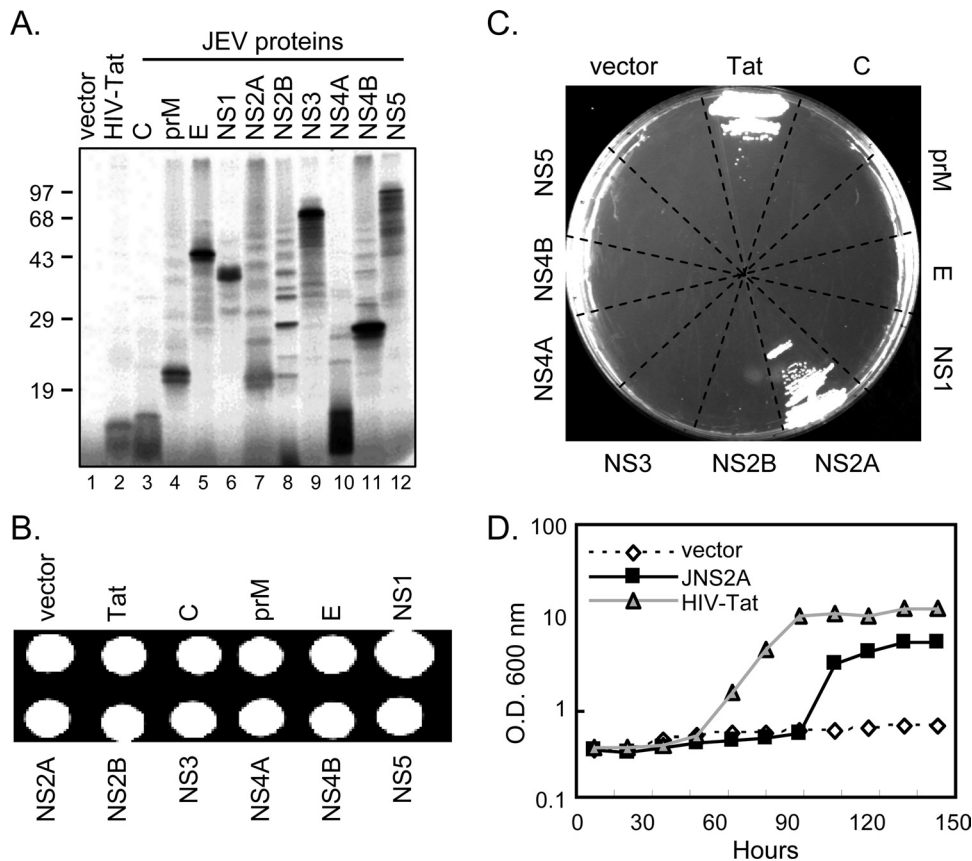
FIG 2 JEV NS2A blocked PKR-mediated growth suppression in PKR-expressing yeast system. (A) Individual cDNAs of JEV viral proteins and HIV Tat were subcloned to pYES2 vector under the GAL1 and T7 promoters. The plasmid protein expression was checked by the T7-coupled TNT rabbit reticulocyte lysate system. Proteins were labeled with [^{35}S]methionine, separated by SDS-PAGE, and analyzed by autoradiography. (B) Growth of yeast RY1-1 transformed with the indicated pYES2 constructs on synthetic dextrose (SD) plate containing 2% glucose. (C) RY1-1 transformants were streaked onto a synthetic galactose (SGAL) plate containing 2% galactose for PKR-mediated growth suppression assay. (D) RY1-1 transformed with pYES2 (vector), JNS2A/pYES2, or HIV Tat/pYES2 were inoculated in SD broth at 30°C overnight and then diluted to OD$_{600}$ of 0.4/ml in SGAL (10% galactose) broth. Yeast growth was monitored by spectrometer (OD$_{600}$) at 30°C for the indicated time periods.

more resistant to cell death triggered by dsRNA activation than control A549 and GFP cells (Fig. 3B). Thus, JEV NS2A appears to counteract the dsRNA-triggered PKR activation in mammalian cells.

Translation inhibition triggered by IFN-α was attenuated by JNS2A. Under stress conditions, translation initiation is globally repressed by the phosphorylation of eIF2α (30). To test the potential of JNS2A to rescue the PKR-mediated translation inhibition, we constructed a bicistronic reporter (Fig. 4A), which contained the firefly luciferase (FLuc) translated in a cap-dependent manner that is sensitive to eIF2α phosphorylation, and the *Renilla* luciferase (RLuc) translated under the control of HCV IRES element, which is resistant to eIF2α phosphorylation (37). The relative luciferase activity of FLuc normalized to that of RLuc represents the level of translation blocked by eIF2α phosphorylation. In both A549 and 293T cells, GFP control cells treated with IFN-α known to induce PKR expression and eIF2α phosphorylation, showed suppression of reporter activity (Fig. 4B and C). In cells with JNS2A expression, the reporter activities were rescued to levels similar to that of PKRΔ6, known to block PKR activation (38, 57). Thus, PKR-mediated translational inhibition triggered by IFN-α could be reversed by JNS2A.

eIF2α phosphorylation triggered by PKR, but not by other eIF2α kinases, was blocked by JNS2A. PKR is one of the four kinases of eIF2α; the others are PKR-like ER kinase (PERK), general control non-derepressible-2 (GCN2), and heme-regulated inhibitor (HRI) (61). To test whether other eIF2α kinases could also be blocked by JNS2A, we used different stimuli such as IFN-α, amino acid starvation, tunicamycin, and sodium arsenite to induce eIF2α phosphorylation triggered by PKR, GCN2, PERK and HRI, respectively (37, 61). As expected, eIF2α phosphorylation triggered by IFN-α, which induces PKR expression, was reduced in cells with JNS2A expression (Fig. 5A). However, eIF2α phosphorylation triggered by other kinases was not affected by JNS2A expression (Fig. 5B, C, and D), demonstrating a specificity of PKR blockage by JNS2A. This notion was further supported by a doxorubicin experiment (Fig. 6). The chemotherapeutic doxorubicin has been shown to promote PKR-mediated cell death, and other eIF2α kinases such as PERK and GCN2 did not contribute to doxorubicin-induced cell death (54). Compared to the GFP control cells, cells with JNS2A expression showed suppressed PKR and eIF2α phosphorylation triggered by doxorubicin (Fig. 6A). Cell death triggered by doxorubicin was also alleviated in cells with JNS2A (Fig. 6B). Thus, JNS2A specifically represses PKR ac-

A.

B.
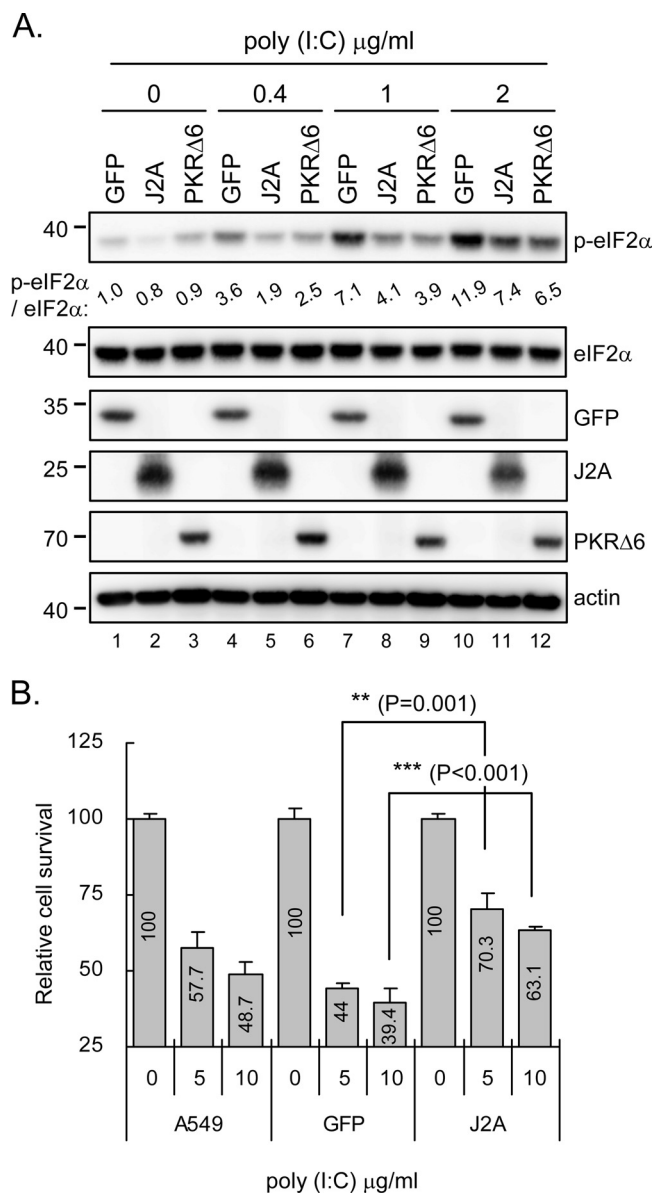
FIG 3 dsRNA-triggered eIF2α phosphorylation and cell death were alleviated by JEV NS2A. (A) Stable A549 cells transduced with lentiviral vectors expressing HA-tagged GFP, JNS2A (J2A), and PKRΔ6 were stimulated with poly(I·C) (0, 0.4, 1, and 2 μg/ml) for 1 h. The cell lysates were then harvested for Western blot analysis with the indicated antibodies. The bands intensities were quantified by MetaMorph (Universal Imaging Corp.), and the relative levels for the indicated proteins are shown. (B) The parental, stable GFP-expressing, and J2A-expressing A549 cells described in panel A were stimulated with poly(I·C) (0, 5, and 10 μg/ml) for 8 h. Viable cell numbers were determined by the trypan blue exclusion method. The relative cell survival of poly(I·C)-treated cells was compared to that without poly(I·C) treatment for each type of cell. The experiment was performed three times with similar results, and representative data from one experiment performed in triplicate are shown with means and the standard deviations (n = 3). **, P < 0.005; ***, P < 0.001 (two-tailed Student t test).

tivation triggered by various stimuli such as dsRNA, IFN-α, and doxorubicin.

Amino acid Thr at residue 33 of JNS2A is important for PKR suppression. HCV NS5A is known to block PKR by binding to the PKR dimerization domain (PKR residues 244 to 296) (23, 26, 33).

A.

B. A549

C. 293T
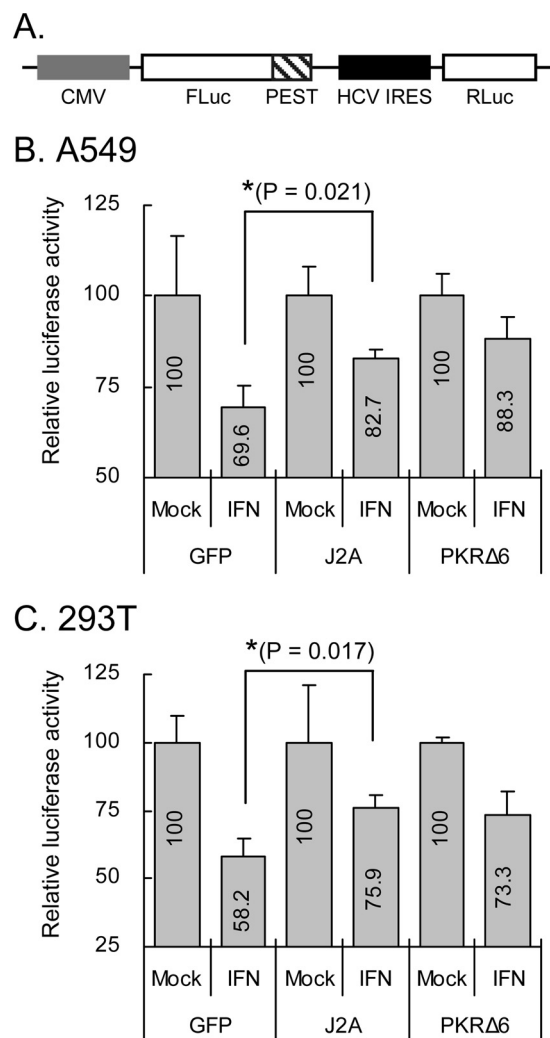
FIG 4 Translation inhibition triggered by IFN-α was attenuated by JNS2A. (A) Schematic representation of the bicistronic reporter CMV-FLuc$_{d2}$-IRES$_{HCV}$-RLuc. A549 (B) and 293T (C) cells cotransfected with the reporter (0.15 μg) plus the plasmids expressing GFP, JNS2A, or PKRΔ6 (0.85 μg) for 24 h were stimulated with IFN-α (2,000 U/ml) for 16 h and then harvested for dual-luciferase assay. FLuc activity was normalized to that of RLuc. The relative luciferase activity was compared between IFN-treated and untreated cells for each transfection group. The experiment was performed three times with similar results, and representative data from one experiment performed in triplicate are shown with means and the standard deviations (n = 3). *, P < 0.05 (two-tailed Student t test).

A region of HCV NS5A (residues 237 to 276 of NS5A) termed ISDR is required for NS5A-PKR interaction (20, 21). Interestingly, we noted a sequence similarity between the PKR dimerization domain, HCV NS5A ISDR, and the N terminus of JNS2A (Fig. 7A). The predominant sequence of HCV NS5A residue Thr-244 has been reported to change from Ile to Thr in an HCV patient before and during IFN therapy (20); we thus tested whether the corresponding sequence Thr-33 in JNS2A might be important for its anti-PKR function. We mutated the JNS2A Thr-33 to Ile (T33I mutation) and established a stable A549 cell line with J2A-T33I overexpression by lentivirus transduction (Fig. 7B). The ability of JNS2A to block the dsRNA-activated PKR and eIF2α phosphorylation was abolished with this T33I mutation (Fig. 7C). Further-
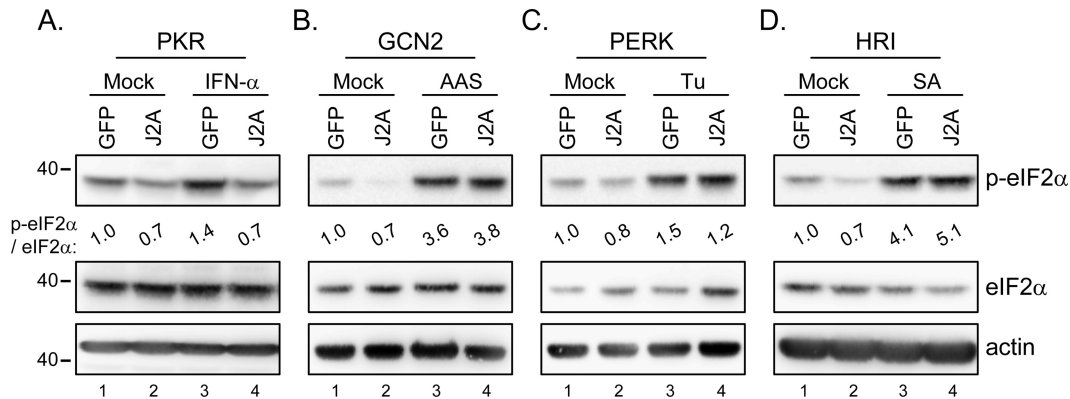
FIG 5 JNS2A specifically suppressed PKR-triggered eIF2α phosphorylation. Stable JNS2A and GFP control cells were exposed to IFN-α (1,000 U/ml for 16 h), amino acid starvation (AAS; cells cultured in PBS for 1 h), tunicamycin (Tu; 2 μg/ml for 1 h), and sodium arsenite (SA; 40 μM for 1 h) to induce eIF2α phosphorylation triggered by PKR (A), GCN2 (B), PERK (C), and HRI (D), respectively. Cell lysates were harvested for Western blotting with the indicated antibodies. The band intensities were quantified by MetaMorph, and the relative levels for the indicated proteins are shown.
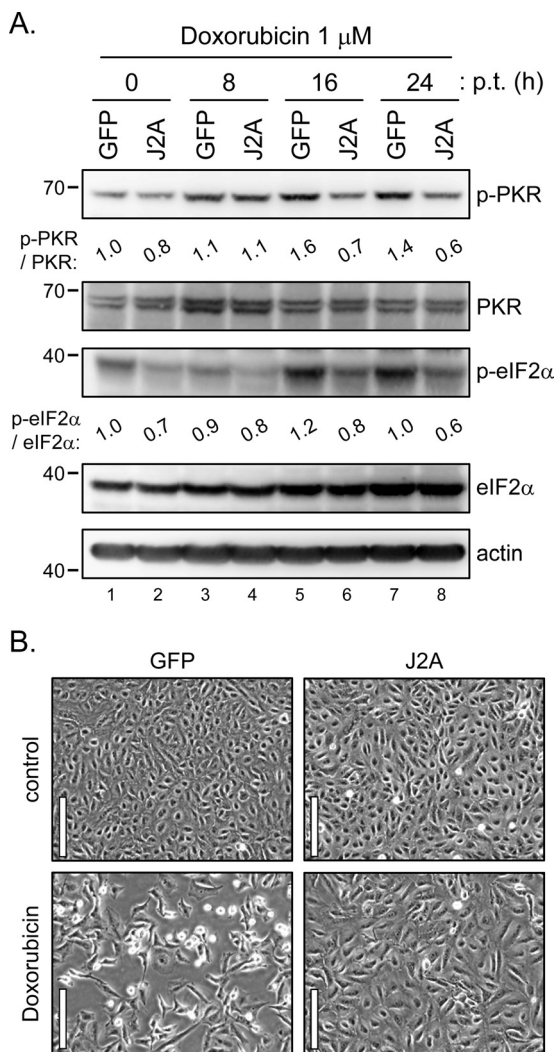

FIG 6 JNS2A reduced the doxorubicin-triggered PKR activation and cell death. (A) Stable JNS2A and GFP control cells treated with doxorubicin (1 μM) for various times were harvested for Western blot analysis with the indicated antibodies. The bands intensities were quantified by MetaMorph, and the relative levels for the indicated proteins are shown. (B) Cell morphology of GFP/A549 and J2A/A549 cells after doxorubicin (1 μM) treatment for 32 h by phase-contrast microscopy. Scale bar, 100 μm.

more, poly(I·C)-triggered IFN-β mRNA induction that depends on PKR activation (31) was lower in cells with JNS2A overexpression compared to that of J2A-T33I and GFP control (Fig. 7D). The cell death measured by annexin V/PI staining also showed that different from the wild-type JNS2A, dsRNA-triggered cell death was not alleviated in cells with J2A-T33I expression (Fig. 7E).

JNS2A interacts with PKR. Because HCV NS5A blocks PKR dimerization and activation by binding to PKR (59), JEV NS2A might also bind to PKR and prevent its activation. To assess this possibility, we used immunoprecipitation-Western blot assay to test whether JNS2A physically interacts with PKR. We cotransfected cells with plasmid expressing Flag-tagged PKRΔ6 to avoid the translational arrest caused by wild-type PKR, plus HA-tagged wild-type J2A or T33I mutant. Immunoprecipitation with anti-HA antibody brought down NS2A, together with PKRΔ6; similarly, anti-Flag antibody immunoprecipitated PKRΔ6 with JNS2A (Fig. 8A). Moreover, reduced interaction with PKR was noted in NS2A-T33I mutant. The interaction between NS2A and PKR is specific, since V5-tagged PKR, but not V5-tagged LacZ, readily pulled down HA-tagged NS2A (Fig. 8B). These data thus suggest that JNS2A might repress PKR activation through a physical interaction with PKR and Thr-33 of NS2A is important for this protein-protein interaction.

NS2A-T33I mutation resulted in a dampened JEV replication phenotype. To further investigate the role of PKR blocking NS2A in the context of JEV infection, we used a JEV RP-9 infectious clone (42) to generate the NS2A-T33I-mutated JEV. Compared to the parental wild-type JEV, the NS2A-T33I mutated virus showed smaller plaque sizes (Fig. 9A), and lower viral progeny production (Fig. 9B). Different from the wild-type JEV infection, higher levels of PKR and eIF2α phosphorylation were noted in cells infected with either one of the two independent clones of NS2A-T33I virus at early time points (8 and 12 h postinfection, Fig. 9C). To verify whether the lower viral growth of NS2A-T33I is indeed due to its defect on antagonizing PKR, we established PKR-knockdown A549 cells (iPKR) by transduction with lentiviral vector expressing shRNA targeting human PKR. NS2A-T33I replicated to higher levels in iPKR cells compared to iLacZ control, as determined by viral progeny production (Fig. 9D) and viral protein expression (Fig. 9E). However, the replication of NS2A-T33I cannot be rescued to a level similar to that of wild-type JEV, sug-
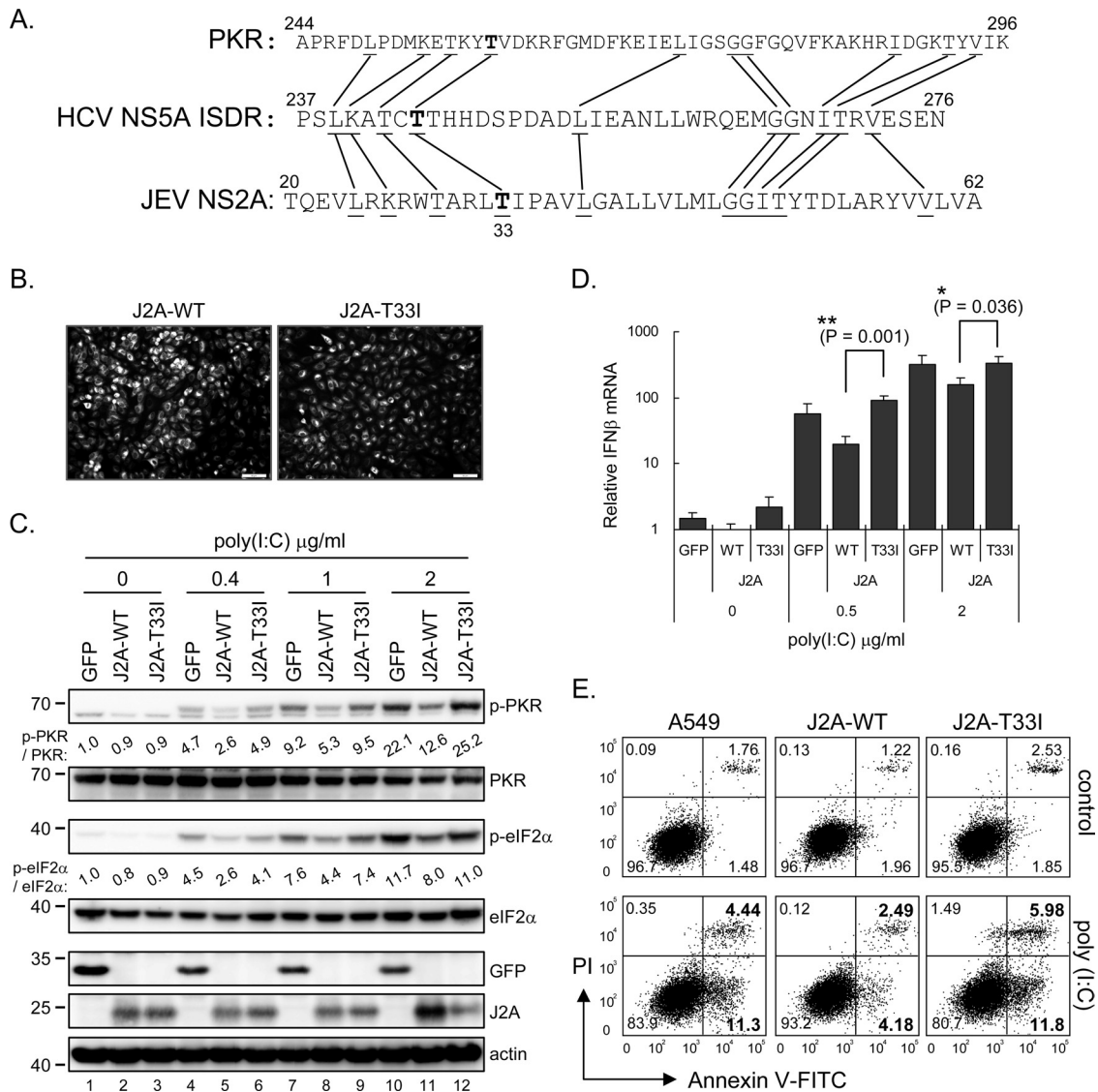
FIG 7 JNS2A-mediated PKR blockage was attenuated by T33I substitution. (A) JNS2A amino acid sequences (residues 20 to 62) were compared to that of PKR dimerization domain (residues 244 to 296) and HCV NS5A ISDR (interferon sensitivity-determining region) (residues 237 to 276). Identical amino acids among these three proteins and the Thr-33 of JNS2A are highlighted by lines and boldfacing, respectively. (B) A JNS2A T33I mutation, a Thr-to-Ile change of NS2A residue 33, was generated by single primer mutation strategy, and stable A549 cells with NS2A-T33I expression were established by lentivirus transduction. The expression of NS2A wild-type (J2A-WT) and T33I mutant (J2A-T33I) in stable cell lines were determined by IFA with anti-HA antibody. (C) Stable A549 cells with HA-tagged GFP, J2A-WT, and J2A-T33I were treated with the indicated doses of poly(I·C) (0, 0.4, 1, and 2 μg/ml) for 1 h and harvested for Western blotting with the indicated antibodies. (D) dsRNA-induced type I IFN production in J2A-WT, J2A-T33I, and GFP control cells was detected by RT-qPCR after poly(I·C) stimulation for 6 h. The relative IFN-β mRNA level was normalized to that of actin ($n = 3$). *, $P < 0.05$; **, $P < 0.005$ (two-tailed Student t test). (E) Flow cytometry of cells stimulated with 2 μg of poly(I·C)/ml for 8 h and then stained with annexin V-FITC and propidium iodide (PI; Biovision). The proportions of cells in each quadrant are shown.

gesting that other functions of NS2A besides PKR repression, such as RNA replication and virus assembly, might also be affected by this mutation. Another possibility is that the residual amount of PKR expression in iPKR cells may still be able to suppress the replication of T33I mutant. The replication of wild-type JEV was also slightly enhanced in iPKR cells, supporting the notion that PKR is an antiviral factor against JEV infection. Furthermore, an induction of PKR expression was noted in iLacZ cells upon NS2A-T33I, but not JEV-WT, infection (Fig. 9E, lanes 1 to 3 and lanes 7 to 9), implying that the repressed PKR blocking of NS2A-T33I

may lead to higher IFN induction and then higher downstream PKR expression.

We further addressed whether the proper anti-PKR function of NS2A contributes to JEV virulence in animals. We noted a lower mortality in mice inoculated with NS2A-T33I mutated virus than the wild-type JEV (Fig. 10A). The levels of viral replication determined by RT-qPCR for JEV viral RNA were higher in the brains of mice inoculated with JEV-WT than in mice inoculated with NS2A-T33I (Fig. 10B). Higher proinflammatory cytokine induction was also noted in mice infected with JEV-WT, as measured by
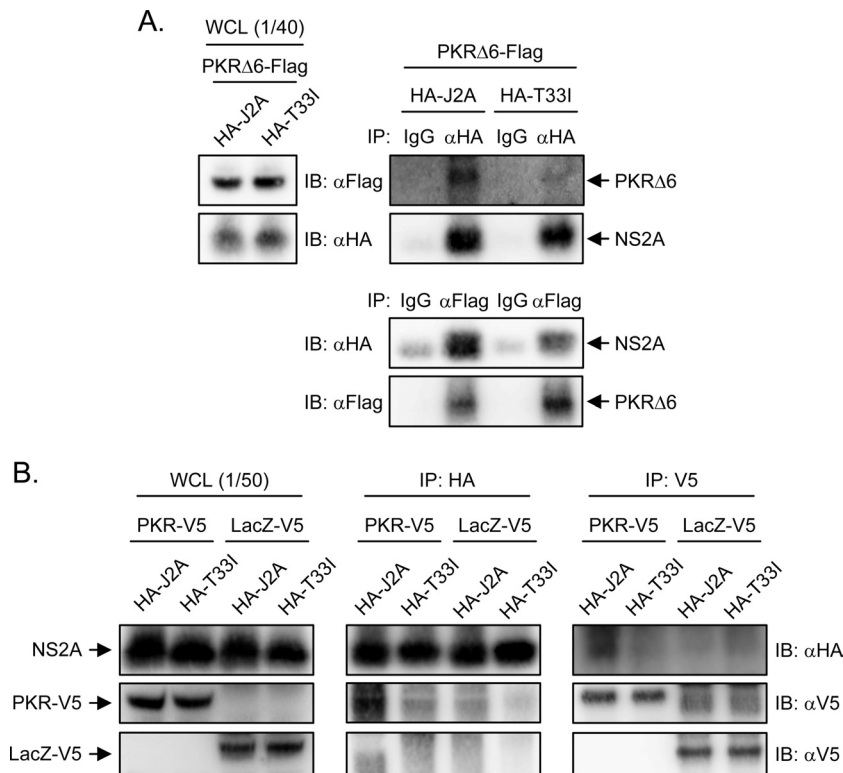
FIG 8 JEV NS2A interacted with PKR. 293T cells were cotransfected with PKRΔ6-Flag plus HA-tagged J2A or T33I for 24 h (A) or PKR-V5 or LacZ-V5 plus HA-tagged J2A or T33I for 24 h (B). The cell lysates were immunoprecipitated with control IgG, anti-HA affinity gel, anti-Flag M2 affinity gel, or anti-V5 antibody as indicated. The immunocomplexes and the whole-cell lysates (WCL) were subjected to Western blot analysis with anti-Flag, anti-HA, or anti-V5 antibodies as indicated.

RT-qPCR for IL-6 mRNA in the brain tissues (Fig. 10C) and by ELISA for IL-6 protein in the sera (Fig. 10D). Infectious virus (~130 PFU/ml) was detected in the sera of mice infected with JEV-WT at day 1 postinfection, but no viremia was detected at day 3 and 5 of JEV-WT infection, nor in the NS2A-T33I-inoculated mice (days 1, 3, and 5 postinfection). However, anti-JEV antibody was readily detected in mice survived from NS2A-T33I challenge (Fig. 10E), suggesting an attenuated phenotype and vaccine potential for JEV with NS2A-T33I mutation. Overall, JEV NS2A was capable of blocking PKR activation, and the proper function of NS2A plays important roles for both *in vitro* and *in vivo* phenotypes of JEV infection.

DISCUSSION

The flaviviral genome is a positive-sense RNA with a 5′ cap but no 3′ poly(A) tail and serves as mRNA for protein translation and a template for RNA replication. Translation of flaviviral RNA is cap dependent and flavivirus infection does not lead to blockage of cellular protein synthesis. PKR activation, which leads to eIF2α phosphorylation and translation inhibition, has been reported as absent (18, 19) or occurring only at a late stage (58) of WNV infection. Similarly, we noted PKR activation only at late stage but not during the early time points of JEV infection. PKR is activated by dsRNA produced during flavivirus RNA replication. Protection of viral RNA by intracellular membrane structures away from the host RNA sensors may be one mechanism to downregulate PKR activation, as reported for WNV infection (13). However, IFN-β gene expression, which is turned on by intracellular sensing

of viral RNA, could be detected as early as 4 to 8 h after JEV infection (8); other mechanisms besides hiding viral RNA inside membrane structures, might also respond for PKR suppression during early stage of JEV infection. Indeed, by rescuing the growth of PKR-expressing yeast, JEV NS2A functioned as an anti-PKR molecule. Furthermore, JEV NS2A also has a PKR-repression effect in human cells stimulated by several PKR activators such as IFN-α, dsRNA, and doxorubicin. Thus, for the first time, a flaviviral protein, JEV NS2A, has been added to the growing list of viral proteins capable of blocking PKR function.

Viruses have evolved various strategies to prevent or overcome the activation of PKR, such as by sequestering its activator dsRNA, by direct binding to the regulatory element of PKR, and by expressing a pseudosubstrate that competes with eIF2α for PKR binding (28, 29). KUNV NS2A can partially colocalize with dsRNA, bind strongly to the 3′ UTR of KUNV RNA (51), and block IFN-β promoter activation (48, 49). Thus, JEV NS2A might bind dsRNA similarly to KUNV NS2A and block PKR activation. In addition, JEV NS2A may function like HCV NS5A to block PKR activation, since we noted amino acid identity between JNS2A, the PKR dimerization domain, and HCV NS5A ISDR (Fig. 7A). HCV NS5A blocks PKR dimerization and activation by binding to the PKR dimerization domain (59). Similarly, JEV NS2A appears to physically interact with PKR (Fig. 8), which might then prevent PKR dimer formation and subsequent activation of PKR. To verify the importance of this region of JNS2A in its anti-PKR potential, we made a single point mutation of residue 33 of NS2A
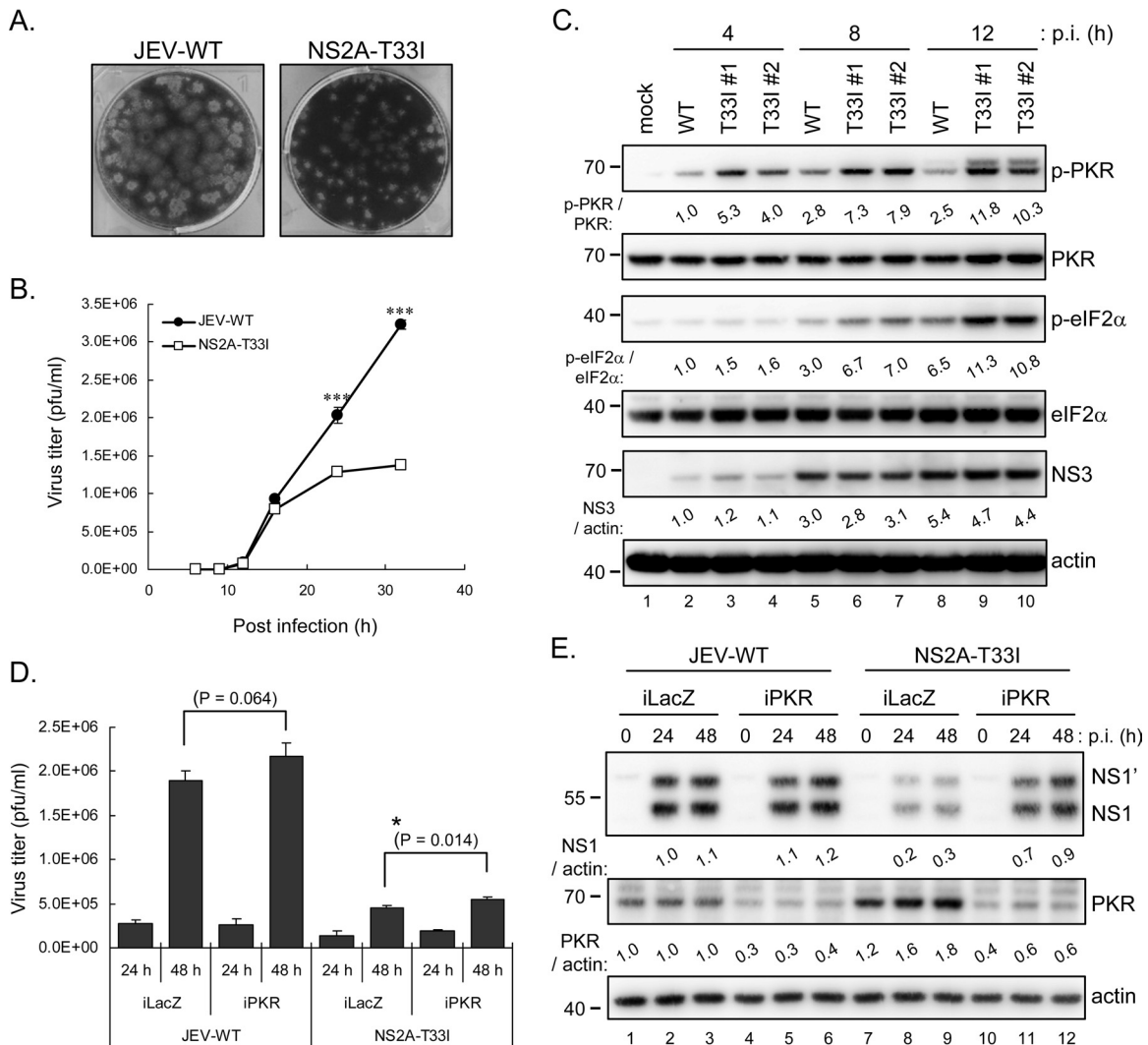
FIG 9 JEV bearing NS2A-T33I mutation replicated to lower levels and was less able to repress PKR activation early during JEV infection. NS2A-T33I-mutated JEV was generated by using a JEV infectious clone as previously described (42). (A) Plaque morphology of JEV wild type (JEV-WT) and NS2A-T33I mutant after 4 days of infection in BHK-21 cells. (B) A549 cells were infected with JEV-WT or NS2A-T33I mutated virus (MOI = 5) for the indicated times. The culture supernatants were collected for virus titration with plaque assays in BHK-21 cells. The experiment was performed three times with similar results, and representative data from one experiment performed in triplicate are shown with means and standard deviations ($n = 3$). (C) Western blot analysis of protein levels in A549 cells infected with JEV-WT or two independent clones of NS2A-T33I mutant (MOI = 5) for the indicated times. (D and E) A549 cells with PKR knockdown (iPKR) or control LacZ knockdown (iLacZ) were infected with JEV-WT or NS2A-T33I (MOI = 0.1) for 24 and 48 h. The culture supernatants were collected for viral titration by plaque assays ($n = 3$) (D), and cell lysates were harvested for Western blotting with antibodies against JEV NS1, PKR, and actin (E). The protein bands intensities were quantified by MetaMorph. *, $P < 0.05$; ***, $P < 0.001$ (two-tailed Student t test).

from Thr to Ile. A change from Ile to Thr in the corresponding residue of HCV NS5A was identified in human HCV infection before and during IFN therapy, which might then contribute to the development of HCV 1b from IFN sensitive to IFN resistant (20). Interestingly, T33I mutation of JNS2A abolished its ability to block PKR activation, suggesting a critical role of Thr-33 of JNS2A in anti-PKR potential. However, the detailed molecular mechanism and other sequence requirements of JEV NS2A to counteract the activation of PKR remain to be studied.

WNV NS2A can block IFN induction and an A30P substitution of WNV NS2A abolished its IFN-suppressing ability (48, 49). The NS2A-A30P-mutated WNV elicited higher levels of IFN-α/β in A549 cells and resulted in abortive infection (49). Because NS2A A30P mutation also disrupts the pseudoknot structure re-

quired for NS1′ expression through a frameshift mechanism (22, 53), it is not clear whether the enhanced IFN induction was resulted from the Ala-to-Pro change of NS2A residue 30 or from the lack of NS1′ expression in this WNV mutant. Other WNV mutants, A30A′ and FSSM, which affect NS1′ expression but not the amino acid sequences of NS2A, have been generated (53). The viral growth in cultured cells and virulence in challenged mice were more profoundly affected by the A30P mutant than by A30A′ and FSSM mutants (53), suggesting that both the expression of NS1′ and the residue 30 of WNV NS2A play a role in viral replication and virulence. Testing whether WNV NS2A can block the activation of PKR and then contribute to IFN suppression (48, 49) is of interest, because PKR can serve as a PRR for WNV-induced IFN production (31). Also of interest is whether the
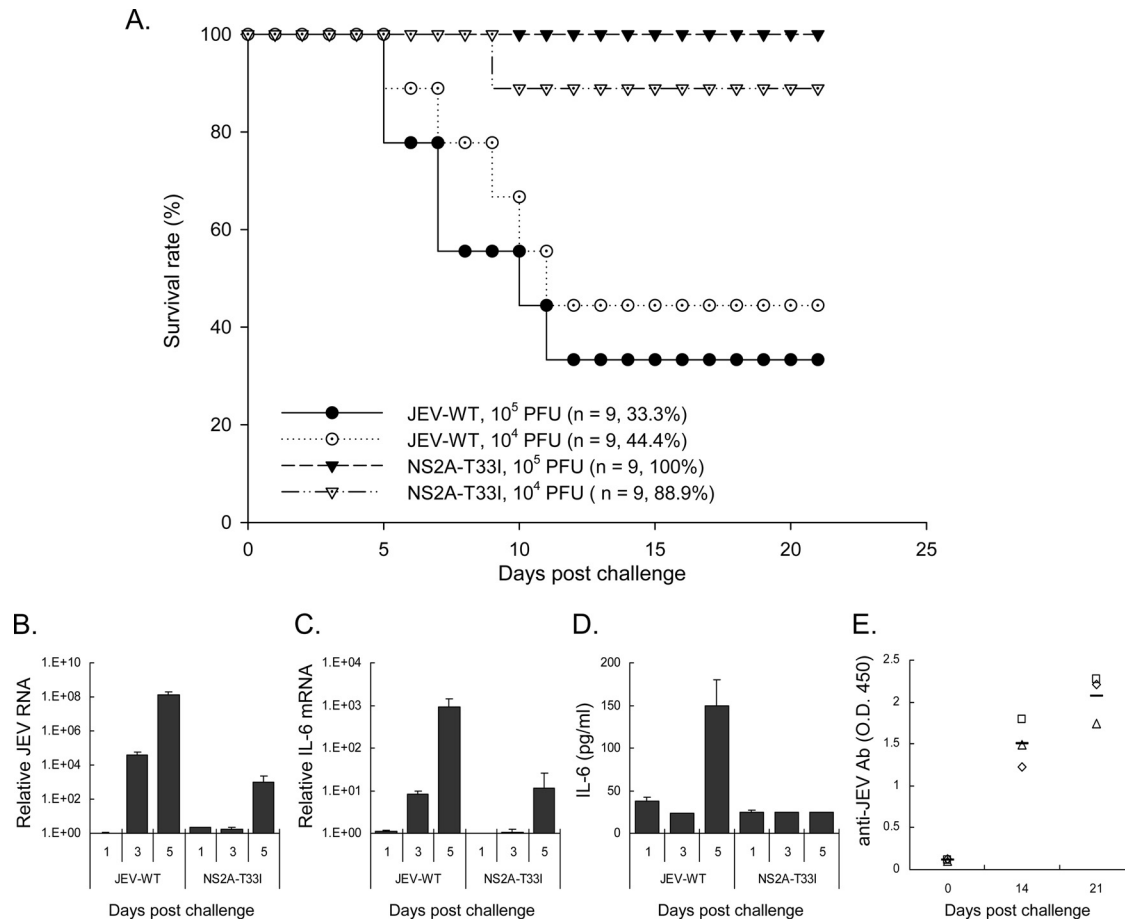
FIG 10 Reduced virulence of NS2A-T33I mutated JEV in challenged mice. (A) Groups of 7-week-old C57BL/6 mice were infected with 10^4 and 10^5 PFU of the wild-type and NS2A-T33I-mutated JEV by IP plus IC route (intraperitoneally inoculation with JEV and intracerebral injection with 30 μl of PBS). Mouse survival was monitored. The animal number (n) and the survival rate for each group are shown. (B) Relative JEV RNA levels in the brain tissues of mice inoculated with JEV-WT or NS2A-T33I (10^5 PFU) were quantified by RT-qPCR ($n = 2$). (C) Relative IL-6 mRNA levels were determined by RT-qPCR with RNA harvested from the brain tissues ($n = 2$). (D) IL-6 protein levels in the serum samples were detected by ELISA at the indicated days postinfection ($n = 2$). (E) The anti-JEV antibody in sera of mice survived from NS2A-T33I infection ($n = 3$) was determined by ELISA.

NS2A-A30P mutation that introduces a Pro residue known to change protein conformation near the Thr-33 residue might damage the anti-PKR potential of JEV NS2A.

JEV with NS2A-T33I substitution can be generated from the mutated infectious clone; however, a growth disadvantage was noted for this mutant JEV. NS2A-T33I-mutated JEV replicated to lower levels and formed smaller plaques compared to the parental wild-type JEV (Fig. 9). Different from the wild-type JEV, which induced low levels of PKR and eIF2α phosphorylation early during infection, the NS2A-T33I mutant virus triggered higher PKR activation in infected cells. Thus, a proper suppression of PKR by NS2A early during infection benefits JEV replication and suggests an antiviral role of PKR in JEV infection. This notion was further extended to the *in vivo* phenotype of JEV in that the T33I mutant was less virulent in challenged mice. The NS2A-T33I mutation did not affect the pseudoknot structure required for NS1′ expression (22, 53), and this mutant JEV still produced NS1 and NS1′ normally (Fig. 9E). Thus, the reduced virulence of the NS2A-T33I mutant is not due to the lack of NS1′ reported to play a role in WNV's neuroinvasiveness (53). A defect in the anti-PKR potential of JEV NS2A-T33I may contribute to its attenuation phenotype in

challenged animals. However, the involvement of other functions of NS2A, such as RNA replication, virus assembly, and inhibition of IFN response, cannot be excluded. These other functions of NS2A might also be affected by T33I mutation and then contribute to lower replication and reduced virulence of JEV-NS2A T33I mutant.

In the present study, we demonstrate a novel function for JEV NS2A in suppressing the cellular antiviral molecule PKR. As reported for other flaviviruses (12, 13, 46), JEV RNA replication is likely biphasic, whereby genomic and complementary minus-strand RNA replicate at low levels until about 10 to 12 h after infection, and then RNA replication increases exponentially with predominantly genomic RNA synthesis. Blocking PKR early during JEV infection by JEV NS2A would blunt the host defense and facilitate viral RNA replication. However, late stages of JEV infection exhibit high levels of PKR phosphorylation, even in the presence of JEV NS2A, so the recognition and activation interplays between PKR and JEV might differ during the biphasic phases of viral replication. Whether the late activation of PKR represents a plethora of viral RNA that inadvertently activates PKR (13) and whether the activated PKR may have an antiviral and/or proviral

role in JEV replication, because both antiviral (31, 35, 36, 58) and proviral (1, 27) roles of PKR have been reported for HCV and flaviviruses, remains elusive. Overall, the fine-tuning of PKR activation in JEV-infected cells would dictate the outcomes of JEV infection.

ACKNOWLEDGMENTS

REFERENCES

1. **Arnaud N, et al.** 2011. Hepatitis C virus reveals a novel early control in acute immune response. PLoS Pathog. **7**:e1002289. doi:10.1371/journal.ppat.1002289.

2. **Arnaud N, et al.** 2010. Hepatitis C virus controls interferon production through PKR activation. PLoS One **5**:e10575. doi:10.1371/journal.pone.0010575.

3. **Balachandran S, Barber GN.** 2007. PKR in innate immunity, cancer, and viral oncolysis. Methods Mol. Biol. **383**:277–301.

4. **Balachandran S, et al.** 1998. Activation of the dsRNA-dependent protein kinase, PKR, induces apoptosis through FADD-mediated death signaling. EMBO J. **17**:6888–6902.

5. **Becker DM, Guarente L.** 1991. High-efficiency transformation of yeast by electroporation. Methods Enzymol. **194**:182–187.

6. **Brand SR, Kobayashi R, Mathews MB.** 1997. The Tat protein of human immunodeficiency virus type 1 is a substrate and inhibitor of the interferon-induced, virally activated protein kinase, PKR. J. Biol. Chem. **272**:8388–8395.

7. **Chang LJ, Urlacher V, Iwakuma T, Cui Y, Zucali J.** 1999. Efficacy and safety analyses of a recombinant human immunodeficiency virus type 1 derived vector system. Gene Ther. **6**:715–728.

8. **Chang TH, Liao CL, Lin YL.** 2006. Flavivirus induces interferon-beta gene expression through a pathway involving RIG-I-dependent IRF-3 and PI3K-dependent NF-κB activation. Microbes Infect. **8**:157–171.

9. **Chen LK, et al.** 1996. Persistence of Japanese encephalitis virus is associated with abnormal expression of the nonstructural protein NS1 in host cells. Virology **217**:220–229.

10. **Chen LK, et al.** 1996. Generation and characterization of organ-tropism mutants of Japanese encephalitis virus in vivo and in vitro. Virology **223**:79–88.

11. **Chong KL, et al.** 1992. Human p68 kinase exhibits growth suppression in yeast and homology to the translational regulator GCN2. EMBO J. **11**:1553–1562.

12. **Chu PW, Westaway EG.** 1985. Replication strategy of Kunjin virus: evidence for recycling role of replicative form RNA as template in semiconservative and asymmetric replication. Virology **140**:68–79.

13. **Courtney SC, Scherbik SV, Stockman BM, Brinton MA.** 2012. West Nile virus infections suppress early viral RNA synthesis and avoid inducing the cell stress granule response. J. Virol. **86**:3647–3657.

14. **Cui Y, Iwakuma T, Chang LJ.** 1999. Contributions of viral splice sites and cis-regulatory elements to lentivirus vector function. J. Virol. **73**:6171–6176.

15. **Der SD, Yang YL, Weissmann C, Williams BR.** 1997. A double-stranded RNA-activated protein kinase-dependent pathway mediating stress-induced apoptosis. Proc. Natl. Acad. Sci. U. S. A. **94**:3279–3283.

16. **Dey M, et al.** 2005. Mechanistic link between PKR dimerization, autophosphorylation, and eIF2α substrate recognition. Cell **122**:901–913.

17. **Diamond MS, Harris E.** 2001. Interferon inhibits dengue virus infection by preventing translation of viral RNA through a PKR-independent mechanism. Virology **289**:297–311.

18. **Elbahesh H, Scherbik SV, Brinton MA.** 2011. West Nile virus infection does not induce PKR activation in rodent cells. Virology **421**:51–60.

19. **Emara MM, Brinton MA.** 2007. Interaction of TIA-1/TIAR with West Nile and dengue virus products in infected cells interferes with stress granule formation and processing body assembly. Proc. Natl. Acad. Sci. U. S. A. **104**:9041–9046.

20. **Enomoto N, et al.** 1995. Comparison of full-length sequences of interferon-sensitive and resistant hepatitis C virus 1b. Sensitivity to interferon is conferred by amino acid substitutions in the NS5A region. J. Clin. Invest. **96**:224–230.

21. **Enomoto N, et al.** 1996. Mutations in the nonstructural protein 5A gene and response to interferon in patients with chronic hepatitis C virus 1b infection. N. Engl. J. Med. **334**:77–81.

22. **Firth AE, Atkins JF.** 2009. A conserved predicted pseudoknot in the NS2A-encoding sequence of West Nile and Japanese encephalitis flaviviruses suggests NS1′ may derive from ribosomal frameshifting. Virol. J. **6**:14.

23. **Gale M, Jr, et al.** 1998. Control of PKR protein kinase by hepatitis C virus nonstructural 5A protein: molecular mechanisms of kinase regulation. Mol. Cell. Biol. **18**:5208–5218.

24. **Gale M, Jr, Katze MG.** 1998. Molecular mechanisms of interferon resistance mediated by viral-directed inhibition of PKR, the interferon-induced protein kinase. Pharmacol. Ther. **78**:29–46.

25. **Gale MJ, Jr, Korth MJ, Katze MG.** 1998. Repression of the PKR protein kinase by the hepatitis C virus NS5A protein: a potential mechanism of interferon resistance. Clin. Diagn. Virol. **10**:157–162.

26. **Gale MJ, Jr, et al.** 1997. Evidence that hepatitis C virus resistance to interferon is mediated through repression of the PKR protein kinase by the nonstructural 5A protein. Virology **230**:217–227.

27. **Garaigorta U, Chisari FV.** 2009. Hepatitis C virus blocks interferon effector function by inducing protein kinase R phosphorylation. Cell Host Microbe **6**:513–522.

28. **Garcia MA, et al.** 2006. Impact of protein kinase PKR in cell biology: from antiviral to antiproliferative action. Microbiol. Mol. Biol. Rev. **70**:1032–1060.

29. **Garcia MA, Meurs EF, Esteban M.** 2007. The dsRNA protein kinase PKR: virus and cell control. Biochimie **89**:799–811.

30. **Gebauer F, Hentze MW.** 2004. Molecular mechanisms of translational control. Nat. Rev. Mol. Cell. Biol. **5**:827–835.

31. **Gilfoy FD, Mason PW.** 2007. West Nile virus-induced interferon production is mediated by the double-stranded RNA-dependent protein kinase PKR. J. Virol. **81**:11148–11158.

32. **Hase T, Dubois DR, Summers PL.** 1990. Comparative study of mouse brains infected with Japanese encephalitis virus by intracerebral or intraperitoneal inoculation. Int. J. Exp. Pathol. **71**:857–869.

33. **He Y, et al.** 2001. Regulation of mRNA translation and cellular signaling by hepatitis C virus nonstructural protein NS5A. J. Virol. **75**:5090–5098.

34. **Iwakuma T, Cui Y, Chang LJ.** 1999. Self-inactivating lentiviral vectors with U3 and U5 modifications. Virology **261**:120–132.

35. **Jiang D, et al.** 2008. Identification of three interferon-inducible cellular enzymes that inhibit the replication of hepatitis C virus. J. Virol. **82**:1665–1678.

36. **Jiang D, et al.** 2010. Identification of five interferon-induced cellular proteins that inhibit West Nile virus and dengue virus infections. J. Virol. **84**:8332–8341.

37. **Kim JH, Park SM, Park JH, Keum SJ, Jang SK.** 2011. eIF2A mediates translation of hepatitis C viral mRNA under stress conditions. EMBO J. **30**:2454–2464.

38. **Koromilas AE, Roy S, Barber GN, Katze MG, Sonenberg N.** 1992. Malignant transformation by a mutant of the IFN-inducible dsRNA-dependent protein kinase. Science **257**:1685–1689.

39. **Kummerer BM, Rice CM.** 2002. Mutations in the yellow fever virus nonstructural protein NS2A selectively block production of infectious particles. J. Virol. **76**:4773–4784.

40. **Leung JY, et al.** 2008. Role of nonstructural protein NS2A in flavivirus assembly. J. Virol. **82**:4731–4741.

41. **Li X, et al.** 1998. Generation of destabilized green fluorescent protein as a transcription reporter. J. Biol. Chem. **273**:34970–34975.

42. **Liang JJ, Liao CL, Liao JT, Lee YL, Lin YL.** 2009. A Japanese encephalitis virus vaccine candidate strain is attenuated by decreasing its interferon antagonistic ability. Vaccine **27**:2746–2754.

43. **Liang JJ, Yu CY, Liao CL, Lin YL.** 2011. Vimentin binding is critical for infection by the virulent strain of Japanese encephalitis virus. Cell Microbiol. **13**:1358–1370.

44. **Lin RJ, Chang BL, Yu HP, Liao CL, Lin YL.** 2006. Blocking of interferon-induced Jak-Stat signaling by Japanese encephalitis virus NS5 through a protein tyrosine phosphatase-mediated mechanism. J. Virol. **80**:5908–5918.

45. **Lin YL, et al.** 1996. A highly attenuated strain of Japanese encephalitis virus induces a protective immune response in mice. Virus Res. **44**:45–56.

46. **Lindenbach BD, Thiel H-J, Rice CM.** 2007. *Flaviviridae*: the viruses and their replication, p 1101–1152. *In* Knipe DM, Howley PM (ed), Fields virology, 5th ed, vol 1. Lippincott/The Williams & Wilkins Co, Philadelphia, PA.

47. **Liu WJ, Chen HB, Khromykh AA.** 2003. Molecular and functional analyses of Kunjin virus infectious cDNA clones demonstrate the essential roles for NS2A in virus assembly and for a nonconservative residue in NS3 in RNA replication. J. Virol. **77**:7804–7813.

48. **Liu WJ, Chen HB, Wang XJ, Huang H, Khromykh AA.** 2004. Analysis of adaptive mutations in Kunjin virus replicon RNA reveals a novel role for the flavivirus nonstructural protein NS2A in inhibition of beta interferon promoter-driven transcription. J. Virol. **78**:12225–12235.

49. **Liu WJ, et al.** 2006. A single amino acid substitution in the West Nile virus nonstructural protein NS2A disables its ability to inhibit alpha/beta interferon induction and attenuates virus virulence in mice. J. Virol. **80**:2396–2404.

50. **Liu WJ, et al.** 2005. Inhibition of interferon signaling by the New York 99 strain and Kunjin subtype of West Nile virus involves blockage of STAT1 and STAT2 activation by nonstructural proteins. J. Virol. **79**:1934–1942.

51. **Mackenzie JM, Khromykh AA, Jones MK, Westaway EG.** 1998. Subcellular localization and some biochemical properties of the flavivirus Kunjin nonstructural proteins NS2A and NS4A. Virology **245**:203–215.

52. **Makarova O, Kamberov E, Margolis B.** 2000. Generation of deletion and point mutations with one primer in a single cloning step. Biotechniques **29**:970–972.

53. **Melian EB, et al.** 2010. NS1′ of flaviviruses in the Japanese encephalitis virus serogroup is a product of ribosomal frameshifting and plays a role in viral neuroinvasiveness. J. Virol. **84**:1641–1647.

54. **Peidis P, Papadakis AI, Muaddi H, Richard S, Koromilas AE.** 2011. Doxorubicin bypasses the cytoprotective effects of eIF2α phosphorylation and promotes PKR-mediated cell death. Cell Death Differ. **18**:145–154.

55. **Pindel A, Sadler A.** 2011. The role of protein kinase R in the interferon response. J. Interferon Cytokine Res. **31**:59–70.

56. **Rogers S, Wells R, Rechsteiner M.** 1986. Amino acid sequences common to rapidly degraded proteins: the PEST hypothesis. Science **234**:364–368.

57. **Romano PR, Green SR, Barber GN, Mathews MB, Hinnebusch AG.** 1995. Structural requirements for double-stranded RNA binding, dimerization, and activation of the human eIF-2α kinase DAI in *Saccharomyces cerevisiae*. Mol. Cell. Biol. **15**:365–378.

58. **Samuel MA, et al.** 2006. PKR and RNase L contribute to protection against lethal West Nile virus infection by controlling early viral spread in the periphery and replication in neurons. J. Virol. **80**:7009–7019.

59. **Tan SL, Katze MG.** 2001. How hepatitis C virus counteracts the interferon response: the jury is still out on NS5A. Virology **284**:1–12.

60. **Taylor DR, Shi ST, Romano PR, Barber GN, Lai MM.** 1999. Inhibition of the interferon-inducible protein kinase PKR by HCV E2 protein. Science **285**:107–110.

61. **Wek RC, Jiang HY, Anthony TG.** 2006. Coping with stress: eIF2 kinases and translational control. Biochem. Soc. Trans. **34**:7–11.

62. **Wu SF, et al.** 2003. Evaluation of protective efficacy and immune mechanisms of using a nonstructural protein NS1 in DNA vaccine against dengue 2 virus in mice. Vaccine **21**:3919–3929.

63. **Yu CY, Hsu YW, Liao CL, Lin YL.** 2006. Flavivirus infection activates the XBP1 pathway of the unfolded protein response to cope with endoplasmic reticulum stress. J. Virol. **80**:11868–11880.

64. **Zhang F, et al.** 2001. Binding of double-stranded RNA to protein kinase PKR is required for dimerization and promotes critical autophosphorylation events in the activation loop. J. Biol. Chem. **276**:24946–24958.